Isolating the Spectroscopic Signature of a Hydration Shell With the Use of Clusters: Superoxide Tetrahydrate

J. Mathias Weber, Jude A. Kelley, Steen B. Nielsen,* Patrick Ayotte,† Mark A. Johnson‡

Cluster spectroscopy, aided by ab initio theory, was used to determine the detailed structure of a complete hydration shell around an anion. Infrared spectra of size-selected $O_2^-\cdot(H_2O)_n$ (n = 1 to 4) cluster ions were obtained by photoevaporation of an argon nanomatrix. Four water molecules are required to complete the coordination shell. The simple spectrum of the tetrahydrate reveals a structure in which each water molecule is engaged in a single hydrogen bond to one of the four lobes of the π^* orbital of the superoxide, whereas the water molecules bind together in pairs. This illustrates how water networks deform upon accommodating a solute ion to create a distinct supramolecular species.

The superoxide anion, O_2^-, is one of the most important diatomic anions in nature. It plays a central role in physiological processes such as aging (*1*) and inflammation (*2*). Although the exact reaction mechanisms are not known, it is clear that even in the hydrophobic regions of the cell, the isolated O_2^- ion is present in coordination with residual water molecules. Indeed, an important component of its activity results from its disproportionation upon reaction with water to form other oxygen-containing, physiologically active radicals such as HOO and OH (*1*). Superoxide is also present as a major anionic charge carrier in the atmosphere, where it is clustered with abundant atmospheric species such as water and carbon dioxide (*3–5*).

Part of the complexity of superoxide hydration arises from the general property that small anions, unlike their cationic counterparts, bind strongly to only one of the two protons in a water molecule, leaving the other free to form networks with other water molecules in the primary hydration shell. Superoxide presents an additional complication because, in contrast to the spherical halide anions [see, e.g., (*6, 7*), and references therein], the extended charge distribution offered by the partially occupied π^* molecular orbital provides a highly structured "template" for ionic hydrogen bonding.

Because the hydration shell is fluxional in aqueous media, it is not generally possible to determine the detailed structure of the local solvation environment in situ. However, because superoxide contains an unpaired electron, electron spin resonance (ESR) studies have been carried out on frozen solutions (*8, 9*). The resulting spin-splitting patterns revealed that only four protons were strongly coupled to the unpaired electron spin, which in turn indicates that the hydration shell is surprisingly small. Although these data alone could not establish the detailed interactions between the water molecules, this information is, in principle, readily contained in the pattern of OH stretching fundamentals in the infrared (IR) spectrum. Unfortunately, such features are completely masked in the condensed phase by overwhelming background absorption from distant water molecules. On the other hand, gas-phase $O_2^-\cdot(H_2O)_n$ cluster ions seem ideally suited for isolation and direct spectroscopic characterization of the hydration shells. Despite yielding important kinetic and thermochemical data (*10*), however, the early promise of clusters in elucidating ion solvation structures has been frustrated by their large (and typically uncharacterized) internal energy content, which effectively "melts" the delicate network of associated water molecules. Recent advances in cluster ion spectroscopy, particularly the development of Ar nanomatrix isolation spectroscopy (*6*), are poised to improve this situation. Here we exploit this method to structurally characterize a complete hydration shell around an anion. In general, we anticipate that clusters with insufficient water molecules to saturate coordination will display many low-lying isomeric forms, *resulting in* broad, complex spectra in the OH stretching region. Upon completion of a shell, however, a unique, quasi-rigid structure should emerge, displaying a much simpler pattern of bands. It is this simplification that we seek in our search for complete solvation shells.

The $O_2^-\cdot(H_2O)_n$ clusters were cooled in argon nanomatrices [up to six Ar atoms attached to the $O_2^-\cdot(H_2O)_n$ cluster ions] to ensure that the water molecules reside close to minimum energy configurations. The spectra were recorded through evaporation of the matrix upon photoexcitation of vibrational resonances in the embedded hydrated ion complex (*6, 7*). Size selection of the cluster ions was achieved with a tandem, time-of-flight photofragmentation mass spectrometer (*11*).

IR spectra were recorded for the first four hydrates of superoxide (Fig. 1). We isolated the 2500 to 3800 cm^{-1} region because it spans the range of OH stretching fundamentals typically encountered in bare and ion-bound water networks (*12–16*). The most interesting feature of the hydrated superoxide spectra is the marked simplification and sharpening of the vibrational bands upon addition of the fourth water molecule (Figs. 1D and 2A). The three smallest hydrates display rather broad bands in the ionic H-bonding region (2800 to 3500 cm^{-1}), which are much more complex, for example, than the sharp structure recovered in the spectra of the first three water molecules bound to the (spherical) halide ions (*6, 7, 13, 17, 18*).

The overall spectroscopic patterns displayed in Fig. 1 are independent of the extent of argon solvation. The fact that the $O_2^-\cdot(H_2O)_{1\text{-}3}$ spectra remain diffuse with three Ar atoms attached indicates either the presence of many low-lying isomers (*19*) or unstable vibrationally excited states. Both these scenarios are likely for clusters with unsaturated coordination. When many low-lying configurations exist, heterogeneous broadening of the spectra can be expected because of the thermal population of isomeric forms even at the low temperature afforded by Ar solvation. Also, because of superoxide's high basicity (*10*), proton transfer should be accessible in the monohydrates and dihydrates upon excitation of the OH stretch fundamentals, as observed in a previous report of the $F^-\cdot H_2O$ spectrum (*18*). Whatever the cause, the breadth and complexity of the $O_2^-\cdot(H_2O)_{1\text{-}3}$ spectra frustrate identification of structural motifs by comparison with ab initio frequencies.

In contrast to the behavior of the smaller clusters, much sharper structure emerges with the addition of the fourth water molecule. This is consistent with the dominance of only one isomeric form that is sufficiently robust to sup-

Sterling Chemistry Laboratory, Yale University, Post Office Box 208107, New Haven, CT 06520–8107, USA.

*Present address: Institute of Physics and Astronomy, Aarhus Center for Advanced Physics, University of Aarhus, Ny Munkegade, DK-8000 Aarhus C, Denmark.
†Present address: Environmental Molecular Sciences Laboratory, Pacific Northwest National Laboratory, Post Office Box 999, Richland, WA 99352, USA.
‡To whom correspondence should be addressed. E-mail: mark.johnson@yale.edu

press excited state dynamics, if it indeed occurs in the $n = 1$ to 3 systems. This is, in turn, the expected behavior of a completed solvation shell where saturation of available binding sites locks each molecule into a local environment, suppressing excited state proton transfer because of the differential solvation afforded by a symmetrical bonding arrangement.

The band pattern of the tetrahydrate (five well-defined vibrational origins) is readily analyzed in the context of a locked configuration. In the case of pseudorigid neutral networks, the mid IR spectra can often be traced to fundamental transitions of specific OH oscillators in the network (*16*). Thus, a similarly rigid $O_2^-\cdot(H_2O)_4$ cluster should give rise to at most eight bands if all of the water molecules were distinct, and fewer bands as these features become degenerate in higher symmetry structures. The relative simplicity of the observed spectrum thus indicates a high-symmetry arrangement. The structural information encoded in the spectrum can be extracted from the empirical trends established in the hydrated halides (*7*). The overall pattern in the tetrahydrate (Fig. 2A) is most like that observed for the halide dihydrates $X^-\cdot(H_2O)_2$ (X = Cl, Br, I) (*6, 7*). The tetrahydrate has been observed in the $I^-\cdot(H_2O)_4$ cluster [see (*20*), and references therein] and has a completely different pattern than that of the superoxide tetrahydrate.

In the spectrally isomorphic $X^-\cdot(H_2O)_2$ systems, the two water molecules attach as an intact dimeric unit, which yields a unique IR signature because of its strong interwater (IW) OH stretching band in the vicinity of 3600 cm^{-1}. The two constituent water molecules are distinct, with one playing the role of a double donor (DD) and the other an acceptor donor (AD). This gives rise to a four-band pattern assigned to two ionic H bonds (IHBs), one IW stretch, and one free OH (F). The free OH on the AD water oscillates at the highest frequency, usually very close to the mean energy of the symmetric and asymmetric stretches of bare H_2O (= 3707 cm^{-1}). The two IHBs oscillate hundreds of wave numbers below and are split apart. This splitting occurs because the AD water molecule is known to strengthen its IHB (i.e., the cooperative effect in H bonding), with a concomitant lowering of its OH (IHB) stretching frequency relative to that of the DD water molecule.

The $O_2^-\cdot(H_2O)_4$ pattern is so similar to that of the halide dihydrates that the bands can be assigned by inspection. The two features at high energy appear in their usual locations for F and IW bands (*6, 7*), and therefore the weak, sharp peak at 3690 cm^{-1} is assigned to the free OH on an AD water molecule, whereas the other, stronger sharp peak at 3615 cm^{-1} is assigned to an IW H bond of a DD water molecule. Both these high-energy features are established in the spectra of the dihydrated and trihydrated superoxide clusters (Fig. 1, B and C) and persist unshifted in the tetrahydrate (Figs. 1D and 2A). The presence of a free OH peak immediately rules out cyclic water networks, which have all OH molecules engaged in IW or ionic bonding. The lowest energy band at 2950 cm^{-1} is assigned to the IHB of an AD water molecule, and the remaining doublet centered at 3300 cm^{-1} is traced to the IHB of a DD water molecule. The doubling of the latter band, with a splitting on the order of 50 to 100 cm^{-1}, is always encountered for bands in this range because of a strong Fermi interaction (interaction energy $H_f \approx$ 30 cm^{-1}) with the 2←0 overtone of the intramolecular bending vibration. Thus, the spectra reveal that the $O_2^-\cdot(H_2O)_4$ cluster behaves as if it consists of two water dimer subunits that are bound effectively independently to the anion.

Given the simplicity of the observed tetrahydrate spectrum, and aided by our empirical observation that the spectral pattern suggests the presence of two effectively independent dimeric water subclusters, we launched an ab initio search for stable structures meeting the observed constraints. The calculations were performed at the B3LYP level [with a 6-311+G(2d,p) basis set (*21*)] and yielded the minimum energy structure shown in Fig. 3. In this structure, two independent water dimers bind to opposite sides of the π^* orbital, with each water molecule having one OH group engaged in a single H bond to one lobe of the partially occupied π^* molecular orbital. The "locking" of the structure at the tetrahydrate rather than at the dihydrate, which can adopt the same bonding motif, presumably arises because, with the opposite side of the anion left uncoordinated, the dihydrate has low-energy isomeric forms that become unavailable upon insertion of the second water dimer.

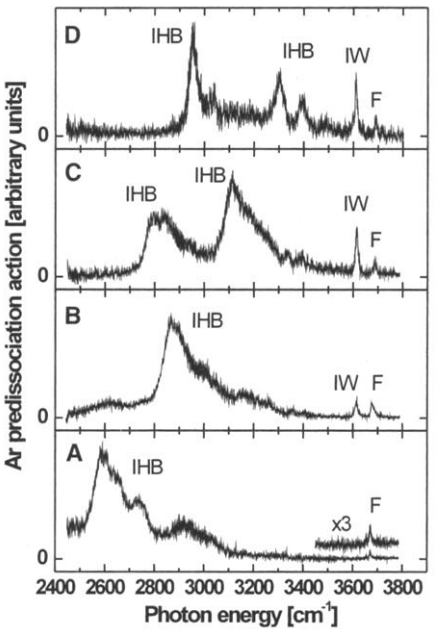

Fig. 1. Ar predissociation spectra of the Ar solvated hydrated superoxide clusters $O_2^-\cdot(H_2O)_n\cdot Ar_3$ (n = 1 to 4). (**A**) Monohydrate (n = 1), (**B**) dihydrate (n = 2), (**C**) trihydrate (n = 3), and (**D**) tetrahydrate (n = 4). Letters denote the H-bonding environments (F, free OH; IW, interwater; IHB, ionic H bond).

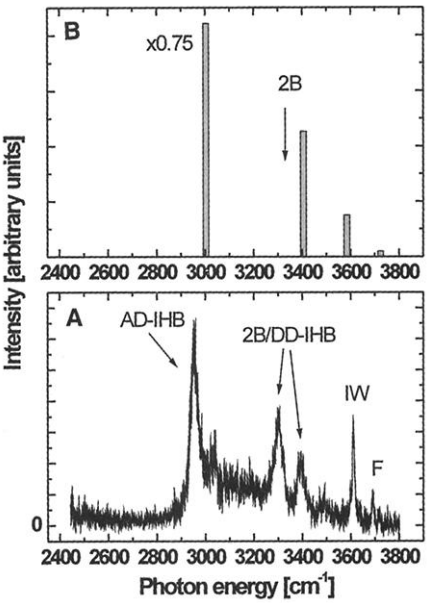

Fig. 2. Calculated and experimental IR spectra of the tetrahydrated superoxide anion. (**A**) Ar predissociation action spectrum of the $O_2^-\cdot(H_2O)_4\cdot Ar_3$ complex. F, free OH group; IW, interwater bond; 2B/DD-IHB, doublet assigned to a bend overtone/IHB-DD Fermi resonance (see text); AD-IHB, donor-acceptor ionic H-bonded stretch. (**B**) Ab initio frequencies for the structure shown in Fig. 3, with the GAUSSIAN 94 program (*21*) on the B3LYP level with a 6-311+G(2d,p) basis set. The frequencies have been scaled for anharmonicity by a factor of 0.96 to match the frequencies of the free water molecule at the same level of theory. The arrow marks the calculated frequency position of the 2←0 overtone of the intramolecular bending mode.

The predicted vibrational spectrum (anharmonicity-corrected fundamentals, Fig. 2B) recovers four fundamentals very close to the experimentally observed positions (Fig. 2A; the predicted band at 3400 cm^{-1} obviously does not anticipate a Fermi resonance). The normal modes arising from the calculation are completely consistent with our empirically extracted assignments. Because of the high symmetry of such a structure, the typical spectral pattern of a cyclic dihydrate is preserved in the tetrahydrate, as the dihydrate motions become collective vibrations of the entire complex and are nearly degenerate. Moreover, only half of the bands are optically allowed in the proposed symmetry.

As noted earlier, the ESR spectrum of frozen solutions revealed that the dominant

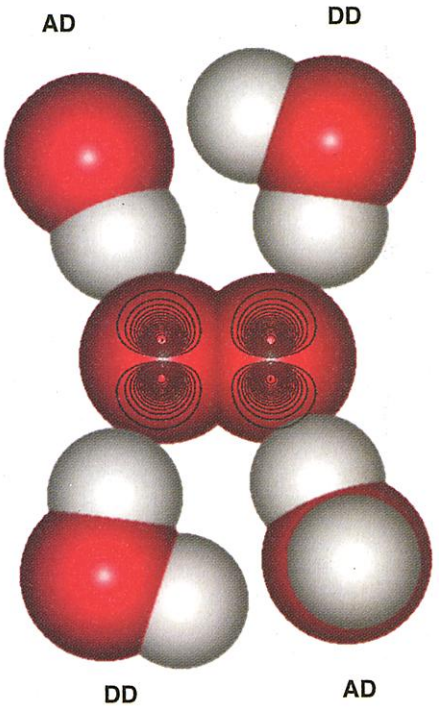

Fig. 3. Calculated minimum energy structure of $O_2^- \cdot (H_2O)_4$. The electron probability density of the π^* orbital is indicated by contours. DD is donor-donor roles and AD is acceptor-donor roles of the constituent water molecules.

interaction with four protons persists in the bulk, just as in our structure of the tetracoordinate hydration shell. Symons *et al.* (*8*) suggested that this saturation upon complexation with only four of the eight available lobes of the degenerate π^* orbital arises because the degeneracy is broken by solvation. This lowers the energy of the configuration where the electron pair occupies the π^* orbital oriented in the plane of the ionic H bonds. It is an open question how these water molecules interact with the higher solvation shells, and this topic is presently being addressed through the study of the larger clusters.

References and Notes

1. C. Schöneich, *Exp. Gerontol.* **34**, 19 (1999).
2. D. Salvemini *et al.*, *Science* **286**, 304 (1999).
3. R. G. Keese, N. Lee, A. W. Castleman Jr., *J. Geophys. Res.* **84**, 3791 (1979).
4. D. W. Fahey, H. Bohringer, F. C. Fehsenfeld, E. E. Ferguson, *J. Chem. Phys.* **76**, 1799 (1982).
5. X. Yang and A. W. Castleman Jr., *J. Am. Chem. Soc.* **113**, 6766 (1991).
6. P. Ayotte, G. H. Weddle, J. Kim, M. A. Johnson, *Chem. Phys.* **239**, 485 (1998).
7. P. Ayotte, S. B. Nielsen, G. H. Weddle, M. A. Johnson, *J. Phys. Chem. A* **103**, 10665 (1999).
8. M. C. R. Symons, G. W. Eastland, L. R. Denny, *J. Chem. Soc. Faraday I* **76**, 1868 (1980).
9. P. A. Narayana, D. Suryanarayana, L. Kevan, *J. Am. Chem. Soc.* **104**, 3552 (1982).
10. W. G. Mallard, Ed., *NIST Standard Reference Database Number 69, Feb. 2000 Release* (Gaithersburg, MD, 1998) (webbook.nist.gov/chemistry).
11. M. A. Johnson and W. C. Lineberger, in *Techniques for the Study of Gas-Phase Ion Molecule Reactions*, J. M. Farrar and W. Saunders, Eds. (Wiley, New York, 1988), pp. 591–635.
12. C. J. Gruenloh *et al.*, *Science* **276**, 1678 (1997).
13. K. T. Kuwata, Y. B. Cao, M. Okumura, *J. Phys. Chem. A* **102**, 503 (1998).
14. P. Ayotte, G. H. Weddle, M. A. Johnson, *J. Chem. Phys.* **110**, 7129 (1999).
15. S. S. Xantheas, *J. Phys. Chem.* **100**, 9703 (1996).
16. J. Sadlej, V. Buch, J. K. Kaziminski, U. Buck, *J. Phys. Chem. A* **103**, 4933 (1999).
17. P. Ayotte, G. H. Weddle, J. Kim, M. A. Johnson, *J. Am. Chem. Soc.* **120**, 12361 (1998).
18. P. Ayotte, J. A. Kelley, S. B. Nielsen, M. A. Johnson, *Chem. Phys Lett.* **316**, 453 (2000).
19. L. A. Curtiss, C. A. Melendres, A. E. Reed, F. Weinhold, *J. Comput. Chem.* **7**, 294 (1986).
20. P. Ayotte, *thesis*, Yale University, New Haven, CT (1999).
21. M. J. Frisch *et al.*, *Gaussian 94, Revision E.1* (Gaussian, Pittsburgh, PA, 1995).

22. We gratefully acknowledge support from the Experimental Physical Chemistry Division of the NSF. We thank W. H. Robertson for valuable technical assistance in the acquisition of data related to this work, and P.A. thanks Fonds pour la Formation de Chercheurs et de l'Aide à la Recherche Bourse Doctorale (FCAR-Québec).

7 December 1999; accepted 10 February 2000

Hot and Dry Deep Crustal Xenoliths from Tibet

Bradley R. Hacker,[1] Edwin Gnos,[2] Lothar Ratschbacher,[3] Marty Grove,[4] Michael McWilliams,[5] Stephen V. Sobolev[6] Jiang Wan,[7] Wu Zhenhan[7]

Anhydrous metasedimentary and mafic xenoliths entrained in 3-million-year-old shoshonitic lavas of the central Tibetan Plateau record a thermal gradient reaching about 800° to 1000°C at a depth of 30 to 50 kilometers; just before extraction, these same xenoliths were heated as much as 200°C. Although these rocks show that the central Tibetan crust is hot enough to cause even dehydration melting of mica, the absence of hydrous minerals, and the match of our calculated *P*-wave speeds and Poisson's ratios with seismological observations, argue against the presence of widespread crustal melting.

The processes that formed the Tibetan Plateau—the highest and largest topographic feature on Earth, and the archetypal signature of continent-continent collision—remain unclear. Models of wholesale underthrusting of India (*1*), lower crustal flow (*2*), intracontinental subduction (*3, 4*), or distributed shortening followed by convective thinning of thickened mantle lithosphere (*5*) make predictions about the thickening, heating, and melting histories of the plateau, but we have little direct knowledge of, for example, the thickness and thermal regime of Tibetan crust during much of the Cenozoic. The ages of crustal extension (*6*), crustal shortening (*7*), rapid upper crustal cooling (*8*), and potassic volcanism (*9*) have all been used to infer when the Tibetan Plateau attained its present thickness of 60 to 75 km, but few studies quantify crustal thickness or thermal gradient. Moreover, the presence of potassic volcanism has been causally linked to convective thinning of overthickened mantle lithosphere—and this seemed a plausible explanation when volcanism appeared to be only 13 million years (My) old and younger. However, recent reports (*10*) reveal that this style of volcanism has occurred in Tibet for 45 My, which calls into question the role of convective thinning, which should be an event with a time scale of about 5 My (*11*). Here we report a detailed analysis of xenoliths from the Tibetan Plateau, which reveal that the lower crust includes anhydrous metasedimentary granulite-facies rocks equilibrated at temperatures of 800° to 1100°C at depths of 30 to 50 km.

Alkalic volcanic rocks have erupted on the Tibetan Plateau since at least 45 million years ago (Ma) (Fig. 1). The most widespread and common are shoshonitic to ultrapotassic trachybasalts to trachytes (*9, 10, 12–14*). Xenoliths and xenocrysts were recently discovered in these volcanic rocks at eight localities (*12, 14, 15*). We examined inclusions from the north-central part of the Qiangtang terrane (*16*) in an area typified by north-south Pliocene-Quaternary grabens (*17*). We observed basaltic flows overlying relatively fresh, porphyritic, trachyandesite to trachyte flows and rhyolites; broad-beam electron-microprobe analyses show that the trachytic flows are moderately shoshonitic (K_2O/Na_2O = 1.5 to 2.0). Phenocrysts in the

[1]Geological Sciences, University of California, Santa Barbara, CA 93106, USA. [2]Mineralogisch-Petrographisches Institut, University of Bern, Baltzerstrasse 1, CH-3012 Bern, Switzerland. [3]Institut für Geologie, Technische Universität Bergakademie Freiberg, Bernhard-von-Cottastrasse 2, D-9596 Freiberg/Sachsen, Germany. [4]Department of Earth and Space Sciences, 3806 Geology Building, Los Angeles, CA 90095–1567, USA. [5]Geological and Environmental Sciences, Stanford University, Stanford, CA 94305–2115, USA. [6]GeoForschungsZentrum Potsdam, Telegrafenberg A17, 14473 Potsdam, Germany. [7]Institute of Geomechanics, Chinese Academy of Geological Sciences, 11 Minzu Xueyuan Nanlu, Beijing, China, 100081.